STRUCTURAL BIOLOGY COMMUNICATIONS

ISSN 2053-230X

Crystal structures of a yeast 14-3-3 protein from *Lachancea thermotolerans* in the unliganded form and bound to a human lipid kinase PI4KB-derived peptide reveal high evolutionary conservation

Andrea Eisenreichova, Martin Klima and Evzen Boura*

Institute of Organic Chemistry and Biochemistry, Academy of Sciences of the Czech Republic, v.v.i., Flemingovo nam. 2, 166 10 Prague 6, Czech Republic. *Correspondence e-mail: evzen.boura@uochb.cas.cz

Received 11 August 2016
Accepted 22 September 2016

Edited by Z. Dauter, Argonne National Laboratory, USA

Keywords: 14-3-3 proteins; Bmh1; Bmh2; crystal structure; phosphopeptide; PI4KB; *Lachancea thermotolerans*.

PDB references: *Lachancea thermotolerans* 14-3-3 protein, apo, 5lho; bound to PI4KB-derived peptide, 5li5

Supporting information: this article has supporting information at journals.iucr.org/f

14-3-3 proteins bind phosphorylated binding partners to regulate several of their properties, including enzymatic activity, stability and subcellular localization. Here, two crystal structures are presented: the crystal structures of the 14-3-3 protein (also known as Bmh1) from the yeast *Lachancea thermotolerans* in the unliganded form and bound to a phosphopeptide derived from human PI4KB (phosphatidylinositol 4-kinase B). The structures demonstrate the high evolutionary conservation of ligand recognition by 14-3-3 proteins. The structural analysis suggests that ligand recognition by 14-3-3 proteins evolved very early in the evolution of eukaryotes and remained conserved, underlying the importance of 14-3-3 proteins in physiology.

1. Introduction

14-3-3 proteins are expressed in every eukaryotic cell and regulate more than 300 binding partners. The interaction is ordinarily regulated by phosphorylation of serine or threonine residues in the R[SFYW]*X*pS*X*P (mode 1) or R*X*[SYFWTQ-AD]*X*p(S/T)*X*[PLM] (mode 2) motifs (where pS and pT denote phosphoserine and phosphothreonine, respectively), but binding to nonphosphorylated ligands has also been reported (Obsil & Obsilova, 2011; Obsilova, Silhan *et al.*, 2008). The binding motifs of 14-3-3 proteins are usually located in the disordered parts or in disordered loops of the binding partners of 14-3-3 proteins (Uhart & Bustos, 2014); therefore, only a handful of crystal structures containing 14-3-3 protein complexes are available. The most prominent examples are the structure of human 14-3-3 protein complexed with serotonin *N*-acetyltransferase (AANAT) and the recent structure of rice 14-3-3 in complex with florigen (Obsil *et al.*, 2001; Taoka *et al.*, 2011).

There are at least two distinct modes of action of 14-3-3 proteins. Perhaps the more common one is the induction of conformational changes in targeted phosphorylated proteins (Obsilova *et al.*, 2014; Rezabkova *et al.*, 2010), supporting the 'molecular anvil hypothesis', in which the rigid 14-3-3 protein mechanically imposes structural changes in target phosphorylated proteins (Yaffe, 2002). Enzymes and proteins acting in signal transduction are usually regulated in this way. For example, in the best studied case of AANAT, 14-3-3ζ modulates the activity and affinity of AANAT by stabilizing a region of AANAT involved in substrate binding (Obsil *et al.*, 2001), which decreases the K_m for 5-hydroxytryptamine (serotonin) and leads to enhanced melatonin production by

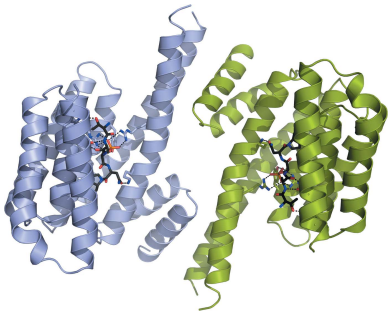

AANAT (Ganguly *et al.*, 2001). However, in the case of nitrate reductase (NR) the 14-3-3 protein induces a conformational change that increases the distance between the two redox-active sites and thus inhibits NR (Lambeck *et al.*, 2012).

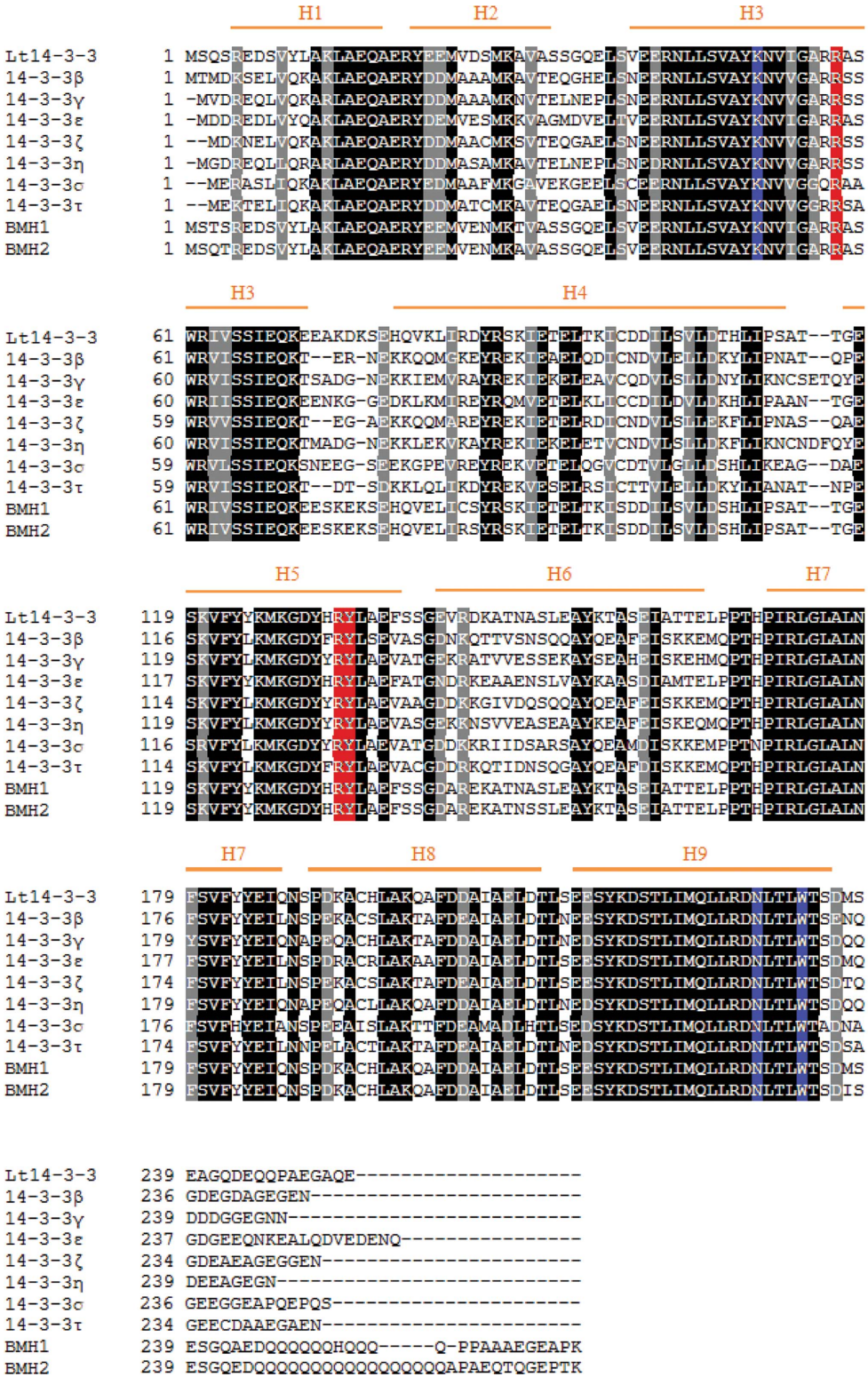

Protein	% identity
14-3-3β	62.45
14-3-3γ	60.39
14-3-3ε	73.54
14-3-3ζ	62.85
14-3-3η	60.00
14-3-3σ	55.69
14-3-3τ	59.68
BMH1	85.77
BMH2	84.25

Figure 1
Sequence similarity of yeast and human 14-3-3 proteins. A multiple sequence alignment of *Lt*14-3-3 with the seven human 14-3-3 isoforms (β, γ, ε, ζ, η, σ and τ) and the *Saccharomyces cerevisiae* 14-3-3 proteins BMH1 and BMH2. The sequence identity of *Lt*14-3-3 to the other 14-3-3 proteins is given. Residues that bind directly to the phosphate group of the PI4KB peptide are highlighted in red and residues that directly bind the PI4KB peptide elsewhere are highlighted in blue.

Changing cellular localization is the other common mode of action of 14-3-3 proteins. For instance, upon binding to the transcription factor FOXO the 14-3-3 protein masks the nuclear localization signal sequence of FOXO transcription factors, which ultimately leads to cytoplasmic localization of FOXO, where it obviously cannot recognize its target DNA sequence (Obsilova *et al.*, 2005; Boura *et al.*, 2010). Additionally, the 14-3-3 protein offers protection from dephosphorylation (Lai *et al.*, 2011; Obsilova, Nedbalkova *et al.*, 2008). PI4KB (phosphatidylinositol 4-kinase B) is a lipid kinase that phosphorylates phosphatidylinositol at position 4 of the inositol ring (Boura & Nencka, 2015), and the 14-3-3 protein has been shown to stabilize its lipid kinase activity *via* protection from dephosphorylation (Hausser *et al.*, 2006).

The structures of all human isoforms of the 14-3-3 protein and of several plant isoforms are known (reviewed in Obsilova *et al.*, 2008). However, the structure of the yeast 14-3-3 protein Bmh1 (brain modulosignalin homologue 1) has not been solved. We were motivated to solve the structure of the yeast 14-3-3 protein Bmh1 in order to obtain further insight into the evolution of 14-3-3 proteins.

2. Materials and methods

2.1. Protein expression and purification

The yeast 14-3-3 protein Bmh1 was amplified from the genomic DNA of *Lachancea thermotolerans* and cloned into a pST39 expression plasmid with an N-terminal His_6 tag and a TEV cleavage site. The protein was purified using standard procedures established in our laboratory (Baumlova *et al.*, 2014; Boura & Hurley, 2012). Briefly, the protein was expressed in *Escherichia coli* BL21 Star cells and lysed in lysis buffer (50 m*M* Tris pH 8, 300 m*M* NaCl, 20 m*M* imidazole, 3 m*M* β-mercaptoethanol, 10% glycerol). Upon affinity chromatography the His_6 tag was cleaved by TEV (*Tobacco etch virus*) protease and Bmh1 was further purified on a Superdex 200 column (GE Healthcare) in SEC buffer (20 m*M* Tris pH 7.4, 100 m*M* NaCl, 3 m*M* β-mercaptoethanol). The protein was concentrated to 8.7 mg ml^{-1} for crystallization trials with unliganded protein and to 5.4 mg ml^{-1} for crystallization trials with peptide-bound Bmh1. The proteins were stored at −80°C until use.

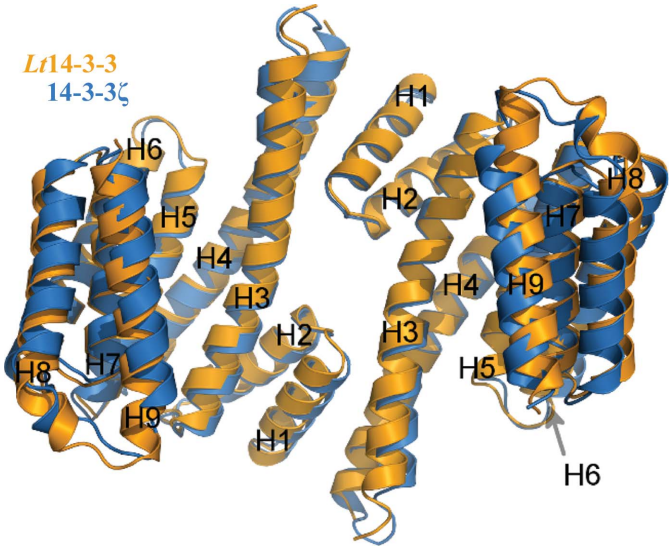

Figure 2
Structural similarity of yeast and human 14-3-3 proteins. *Lt*14-3-3 superposed on human 14-3-3ζ. *Lt*14-3-3 is shown in yellow and 14-3-3ζ in blue. The r.m.s.d. value is 0.79 Å.

Table 1
Statistics of crystallographic data collection and refinement.

Values in parentheses are for the outer shell.

Crystal	Unliganded 14-3-3 protein	PI4KB peptide-bound 14-3-3 protein
Data collection		
X-ray source	MX beamline 14.1, BESSY II	MX beamline 14.1, BESSY II
Wavelength (Å)	0.976	0.918
Space group	$P2_12_12$	$P2_12_12$
Unit-cell parameters (Å)	a = 64.12, b = 122.78, c = 39.17	a = 64.06, b = 123.67, c = 38.68
Resolution (Å)	44.34–1.95 (2.02–1.95)†	44.49–2.58 (2.67–2.58)‡
No. of unique reflections	23282 (2263)	7994 (758)
$\langle I/\sigma(I)\rangle$	14.26 (1.48)	6.50 (1.56)
R_{merge}	0.092 (1.323)	0.1671 (1.045)
Data completeness (%)	99.91 (99.96)	98.35 (98.25)
Multiplicity	8.4 (8.7)	3.9 (4.1)
$CC_{1/2}$	0.999 (0.617)	0.989 (0.506)
Refinement		
R_{work} (%)	18.92 (27.60)	20.17 (28.43)
R_{free} (%)	22.33 (30.25)	25.91 (32.63)
R.m.s.d., bond lengths (Å)	0.012	0.004
R.m.s.d., bond angles (°)	1.21	0.73
Ramachandran		
Outliers (%)	0	0
Favoured (%)	98	99

† $I/\sigma(I)$ = 2 at 2.02 Å resolution. ‡ $I/\sigma(I)$ = 2 at 2.61 Å resolution.

2.2. Crystallization and structural analysis

The unliganded crystals grew at 293 K in a hanging drop created by mixing 1 µl protein solution with 1 µl well solution (13% PEG 3350, 190 m*M* $CaCl_2$, 3% glycerol) and equilibrated by vapour diffusion. The crystals were cryoprotected in well solution supplemented with 35% glycerol and were flash-cooled in liquid nitrogen. They belonged to the orthorhombic space group $P2_12_12$ and diffracted to 2.0 Å resolution. To obtain the structure of the complex, PI4KB peptide was added in a fivefold molar excess. The crystals were grown in a sitting drop by mixing 220 nl protein solution and 220 nl well solution (18% PEG 3350, 180 m*M* magnesium acetate, 20% glycerol). The crystals were flash-cooled in liquid nitrogen. They also belonged to space group $P2_12_12$ and diffracted to 2.8 Å resolution.

Data were collected on the MX-14.1 beamline at BESSY (Mueller *et al.*, 2012), cut based on the $CC_{1/2}$ correlation coefficient and integrated using *XDSAPP* (Krug *et al.*, 2012). The structures were solved using molecular replacement in *Phaser* (McCoy *et al.*, 2007). A previously crystallized 14-3-3 protein (PDB entry 1a4o; Liu *et al.*, 1995) was used as a search model for the unliganded structure. The refined unliganded

structure was subsequently used as a model for the peptide-bound structure. The structures were refined in *PHENIX* (Adams *et al.*, 2010) and *Coot* (Emsley *et al.*, 2010) to good *R* factors and geometry, as summarized in Table 1.

3. Results and discussion

The sequence of the *L. thermotolerans* 14-3-3 protein (*Lt*14-3-3) is similar to the primary sequence of the *Saccharomyces cerevisiae* 14-3-3 protein and to all of the human isoforms (Fig. 1). Therefore, as expected, the overall fold is the same. 14-3-3 proteins consist of nine helices (H1–H9), where the subsequent helix always packs in an antiparallel manner against the preceding helix to create a central binding groove (Fig. 2). The entire protein was clearly visible except for the loop between helices H3 and H4 (Lys70–Glu78), where no density was visible for side chains, and the final 19 C-terminal residues (Ser235–Glu253), which were not visible at all. Superposition of the *Lt*14-3-3 protein onto human 14-3-3ζ revealed high conservation of the ligand-binding groove and the dimer interface, while helices H7, H8 and H9 were somewhat shifted (Fig. 2). The r.m.s.d. to the structurally closest homologue 14-3-3τ (PDB entry 2btp; Yang *et al.*, 2006) was 0.70 Å.

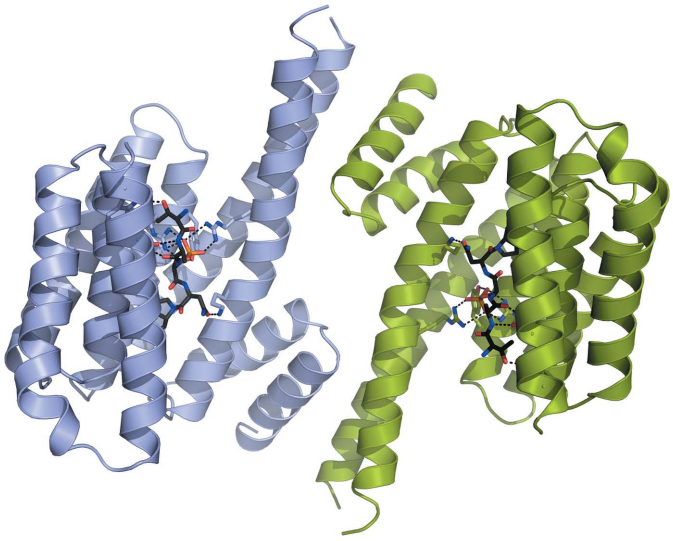

Figure 3
Human PI4KB phosphopeptide bound to the *Lt*14-3-3 dimer. One 14-3-3 monomer is shown in grey and the other in green. The PI4KB peptide is shown in stick representation.

It has been suggested previously that the C-termini of 14-3-3 proteins play an autoinhibitory role by occupying the central binding groove and competing with the phosphorylated binding partner (Silhan *et al.*, 2004). However, this has yet to be observed directly in a crystal structure. Given that *L. thermotolerans* is a thermophile and that proteins from thermophiles are often more rigid, we expected to find the C-terminus in the binding groove. However, we did not observe any density in the central binding groove. Thus, we were not able to crystallographically validate the autoinhibitory hypothesis of Silhan and coworkers.

Since the structure of 14-3-3 proteins has been remarkably conserved through evolution, we postulated that the yeast 14-3-3 protein might be able to bind human protein-derived ligands. Crystallography has become an increasingly utilized tool for analyzing ligand binding (Schiebel *et al.*, 2016; Mejdrová *et al.*, 2015); therefore, we synthesized a peptide derived from human PI4KB lipid kinase (289-LKRTA-pSNPKV-298) that is known to interact with the 14-3-3 protein in human cells (Hausser *et al.*, 2005, 2006). The peptide was mixed with *Lt*14-3-3 in a fivefold molar excess and screened for crystallization. We obtained crystals that diffracted X-rays

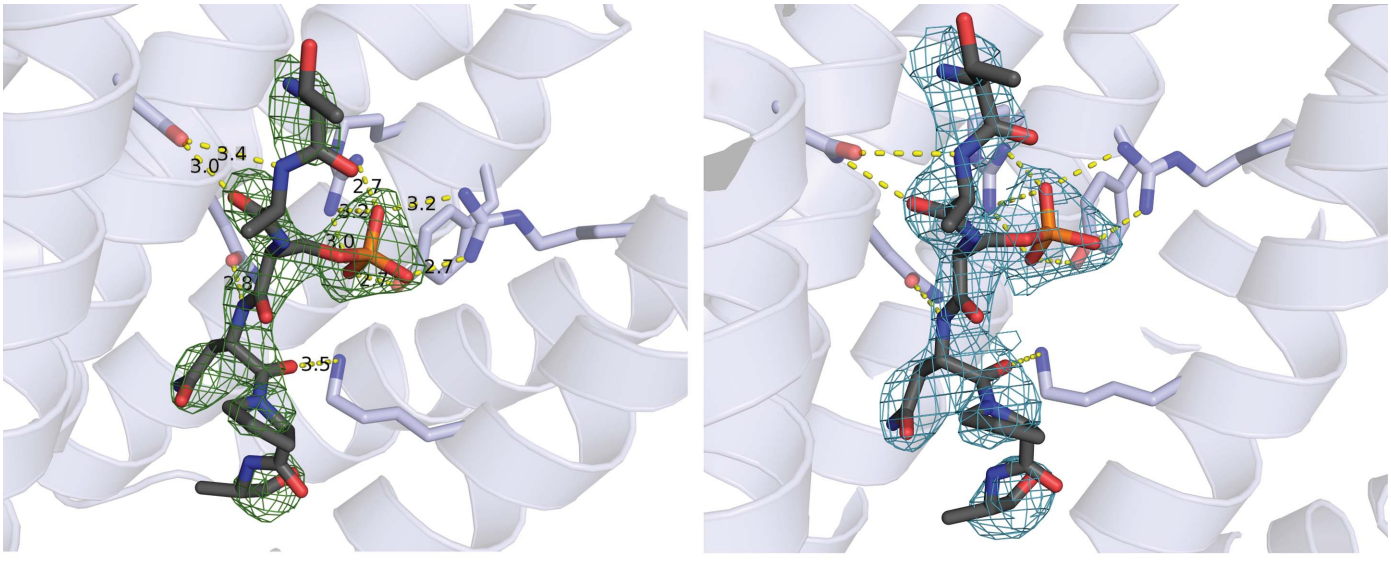

Figure 4
Detailed view of the PI4KB phosphopeptide bound in the central *Lt*14-3-3 binding groove. Amino-acid residues involved in the interaction are represented as sticks; 14-3-3 is coloured grey and the PI4KB phosphopeptide is shown in stick representation. (*a*) The unbiased OMIT $F_o - F_c$ map is coloured green and contoured at 3σ. (*b*) The $2F_o - F_c$ map is coloured blue and contoured at 1σ.

well, albeit to a somewhat lower resolution than the unliganded crystals (2.0 Å *versus* 2.6 Å). Upon molecular replacement, density for the PI4KB peptide was immediately visible; however, we could only model 292-TApSNPK-297 and the rest of the peptide was disordered. The binding mode was adequate for the binding of human 14-3-3 proteins to peptides (Fig. 3), with an r.m.s.d. of 0.43 Å for the unliganded and bound structures. The interaction of the PI4KB peptide with *Lt*14-3-3 is mediated by ionic bonds between the phosphopeptide phosphate group and Arg58, Arg132 and Tyr133 of *Lt*14-3-3 and hydrogen bonds between Lys51, Asn229 and Trp233 of *Lt*14-3-3 and Asn295, Ala293 and Thr292 of the PI4KB phosphopeptide (Fig. 4).

All of the residues that bind the PI4KB phosphopeptide are unequivocally conserved (Figs. 1 and 2). This structurally explains why the yeast 14-3-3 protein is able to bind a human peptide. However, the density for the protein was not as well resolved as in a typical human 14-3-3 protein–human peptide complex and, furthermore, the crystals with the peptide bound diffracted to a 0.6 Å lower resolution, suggesting that ligand binding does not stabilize the *Lt*14-3-3 protein as would be expected. However, the binding mode is conserved and the structures clearly demonstrate high evolutionary conservation of ligand recognition by 14-3-3 proteins. We conclude that ligand recognition by 14-3-3 proteins evolved very early in the evolution in the common ancestor of yeast and humans and has been sustained throughout evolution. Unfortunately, even when using 14-3-3 protein from a thermostable organism we were not able to observe the C-terminus of the protein. Notably, the C-terminus is not conserved at all, suggesting that its previously reported autoinhibitory function is likely to be a specific case that is valid only for the human 14-3-3ζ isoform.

Acknowledgements

We are grateful to the MX beamline 14-1 operated by the Helmholtz-Zentrum Berlin (HZB) at the BESSY II electron-storage ring, where the data were collected. This project was supported by Project InterBioMed LO1302 from the Ministry of Education of the Czech Republic.

References

Adams, P. D. *et al.* (2010). *Acta Cryst.* D**66**, 213–221.
Baumlova, A., Chalupska, D., Różycki, B., Jovic, M., Wisniewski, E., Klima, M., Dubankova, A., Kloer, D. P., Nencka, R., Balla, T. & Boura, E. (2014). *EMBO Rep.* **15**, 1085–1092.
Boura, E. & Hurley, J. H. (2012). *Proc. Natl Acad. Sci. USA*, **109**, 1901–1906.
Boura, E. & Nencka, R. (2015). *Exp. Cell Res.* **337**, 136–145.
Boura, E., Rezabkova, L., Brynda, J., Obsilova, V. & Obsil, T. (2010). *Acta Cryst.* D**66**, 1351–1357.
Emsley, P., Lohkamp, B., Scott, W. G. & Cowtan, K. (2010). *Acta Cryst.* D**66**, 486–501.
Ganguly, S., Gastel, J. A., Weller, J. L., Schwartz, C., Jaffe, H., Namboodiri, M. A., Coon, S. L., Hickman, A. B., Rollag, M., Obsil, T., Beauverger, P., Ferry, G., Boutin, J. A. & Klein, D. C. (2001). *Proc. Natl Acad. Sci. USA*, **98**, 8083–8088.
Hausser, A., Link, G., Hoene, M., Russo, C., Selchow, O. & Pfizenmaier, K. (2006). *J. Cell Sci.* **119**, 3613–3621.
Hausser, A., Storz, P., Märtens, S., Link, G., Toker, A. & Pfizenmaier, K. (2005). *Nature Cell Biol.* **7**, 880–886.
Krug, M., Weiss, M. S., Heinemann, U. & Mueller, U. (2012). *J. Appl. Cryst.* **45**, 568–572.
Lai, S., O'Callaghan, B., Zoghbi, H. Y. & Orr, H. T. (2011). *J. Biol. Chem.* **286**, 34606–34616.
Lambeck, I. C., Fischer-Schrader, K., Niks, D., Roeper, J., Chi, J.-C., Hille, R. & Schwarz, G. (2012). *J. Biol. Chem.* **287**, 4562–4571.
Liu, D., Bienkowska, J., Petosa, C., Collier, R. J., Fu, H. & Liddington, R. (1995). *Nature (London)*, **376**, 191–194.
McCoy, A. J., Grosse-Kunstleve, R. W., Adams, P. D., Winn, M. D., Storoni, L. C. & Read, R. J. (2007). *J. Appl. Cryst.* **40**, 658–674.
Mejdrová, I. *et al.* (2015). *J. Med. Chem.* **58**, 3767–3793.
Mueller, U., Darowski, N., Fuchs, M. R., Förster, R., Hellmig, M., Paithankar, K. S., Pühringer, S., Steffien, M., Zocher, G. & Weiss, M. S. (2012). *J. Synchrotron Rad.* **19**, 442–449.
Obsil, T., Ghirlando, R., Klein, D. C., Ganguly, S. & Dyda, F. (2001). *Cell*, **105**, 257–267.
Obsil, T. & Obsilova, V. (2011). *Semin. Cell Dev. Biol.* **22**, 663–672.
Obsilova, V., Kopecka, M., Kosek, D., Kacirova, M., Kylarova, S., Rezabkova, L. & Obsil, T. (2014). *Physiol. Res.* **63**, S155–S164.
Obsilova, V., Nedbalkova, E., Silhan, J., Boura, E., Herman, P., Vecer, J., Sulc, M., Teisinger, J., Dyda, F. & Obsil, T. (2008). *Biochemistry*, **47**, 1768–1777.
Obsilova, V., Silhan, J., Boura, E., Teisinger, J. & Obsil, T. (2008). *Physiol. Res.* **57**, S11–S21.
Obsilova, V., Vecer, J., Herman, P., Pabianova, A., Sulc, M., Teisinger, J., Boura, E. & Obsil, T. (2005). *Biochemistry*, **44**, 11608–11617.
Rezabkova, L., Boura, E., Herman, P., Vecer, J., Bourova, L., Sulc, M., Svoboda, P., Obsilova, V. & Obsil, T. (2010). *J. Struct. Biol.* **170**, 451–461.
Schiebel, J., Radeva, N., Krimmer, S. G., Wang, X., Stieler, M., Ehrmann, F. R., Fu, K., Metz, A., Huschmann, F. U., Weiss, M. S., Mueller, U., Heine, A. & Klebe, G. (2016). *ACS Chem. Biol.* **11**, 1693–1701.
Silhan, J., Obsilova, V., Vecer, J., Herman, P., Sulc, M., Teisinger, J. & Obsil, T. (2004). *J. Biol. Chem.* **279**, 49113–49119.
Taoka, K., Ohki, I., Tsuji, H., Furuita, K., Hayashi, K., Yanase, T., Yamaguchi, M., Nakashima, C., Purwestri, Y. A., Tamaki, S., Ogaki, Y., Shimada, C., Nakagawa, A., Kojima, C. & Shimamoto, K. (2011). *Nature (London)*, **476**, 332–335.
Uhart, M. & Bustos, D. M. (2014). *Front. Genet.* **5**, 10.
Yaffe, M. B. (2002). *FEBS Lett.* **513**, 53–57.
Yang, X., Lee, W. H., Sobott, F., Papagrigoriou, E., Robinson, C. V., Grossmann, J. G., Sundstrom, M., Doyle, D. A. & Elkins, J. M. (2006). *Proc. Natl Acad. Sci. USA*, **103**, 17237–17242.